Universal grazing bifurcations in impact oscillators

Fernando Casas,* Wai Chin,† Celso Grebogi,†,‡ and Edward Ott§
Institute for Plasma Research, University of Maryland, College Park, Maryland 20742
(Received 5 September 1995)

We examine the bifurcations of a piecewise smooth map that captures the universal properties of impact oscillators near grazing. In particular, we study periodic orbits with one impact per period and the way they are involved in the grazing bifurcations. We also show some phenomena that these orbits exhibit at grazing for some families of parameter values.

PACS number(s): 05.45.+b

I. INTRODUCTION

In the past few years there has been a growing interest in the study of the so-called impact oscillators. These arise whenever the components of an oscillator collide with each other or with rigid obstacles, and occur in many physical applications such as mechanical devices, relaxation oscillators, and electronics. Impact oscillators constitute a subclass of the dynamical systems that do not satisfy the usual smoothness assumptions. More specifically, they are modeled by piecewise continuously differentiable maps. Although great progress has been made in understanding the dynamics of impact oscillators, the complexity and variety of the dynamical phenomena produced by the presence of discontinuities in the system are such that additional studies are necessary, and more examples have to be considered.

One of the aspects that has received much attention in the literature in the recent past is the effect of grazing impacts (i.e., zero velocity impacts) on the dynamics of impact oscillators [1–3], in particular the existence of the so-called grazing bifurcations observed at grazing [4,5].

In this paper we study this kind of bifurcations for the Nordmark map $(x_{n+1},y_{n+1})=F_\rho(x_n,y_n)$ [6,7], with

$$F_\rho(x,y)=\begin{cases}(\alpha x+y+\rho,-\gamma x) & \text{for } x\le 0\\ (-\sqrt{x}+y+\rho,-\gamma\tau^2 x) & \text{for } x>0\ .\end{cases} \tag{1}$$

This is a particular example of a piecewise smooth map from $\mathbb{R}^2$ into itself that models the behavior of a sinusoidally forced linear oscillator experiencing impacts at a hard wall (see Fig. 1). It is obtained by expanding (to first order) solutions of the system in the neighborhood of a grazing orbit [6], so the map is expected to capture the universal properties of the dynamics near grazing. The equivalence with the physical system is established as follows: x_n and y_n are transformed coordinates in the position-velocity space $(\xi,\dot{\xi})$ of the impact oscillator evaluated at times $t_n=2n\pi/\omega$, where ω is the frequency of the external forcing. The quantity τ^2 is the restitution coefficient of the impacts, whereas ρ is related to the amplitude of the external force. The parameters α and γ depend on the intrinsic properties of the oscillator in such a way that the limit $\gamma\to 0$ corresponds to large friction coefficients, and $\gamma\tau^2=1$ gives the opposite limit of zero dissipation, and for physically admissible systems (i.e., positive friction) we have

$$0<\gamma<1,\quad -2\sqrt{\gamma}<\alpha<1+\gamma\ . \tag{2}$$

The first of Eqs. (1) governs the system if there is no impact between time t_n and t_{n+1}. Otherwise, if an impact takes place between t_n and t_{n+1}, the system is described by the second equation. Thus the effect of impacts is modeled by a square root nonlinearity.

The Nordmark map is continuously differentiable except at $x=0$, where its Jacobian matrix is singular. This singularity is responsible for interesting bifurcation phenomena [7,8]. In this system the grazing state corresponds to $\rho=0$, and therefore grazing bifurcations occur as the parameter ρ is increased through $\rho=0$, with γ and α held fixed. These bifurcations have been studied for the system (1) for $0<\alpha<1+\gamma$ in Ref. [7]. There are three basic bifurcation scenarios that have been analyzed, and the corresponding regions in the (γ,α) parameter space where these scenarios take place have been established. Thus, in region I $(2\sqrt{\gamma}<\alpha<\frac{3}{2}\gamma+\frac{2}{3})$ there are grazing bifurcations from a stable period-1 attractor to a reversed infinite period adding cascade, systems in region II

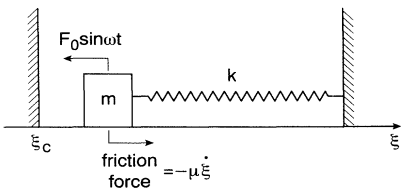

FIG. 1. Physical system modeled by the Nordmark map near grazing.

*Permanent address: Departament de Matemàtiques, Universitat Jaume I, 12071-Castellón, Spain.

†Also at the Department of Mathematics.

‡Also at the Institute for Physical Science and Technology.

§Also at the Department of Physics, Department of Electrical Engineering, and Institute for Systems Research.

($\frac{3}{2}\gamma+\frac{2}{3}<\alpha<1+\gamma$) have bifurcations from a stable period-1 orbit in $\rho<0$ to a chaotic attractor as ρ increases through zero, and systems in region III ($0<\alpha<2\sqrt{\gamma}$) experience local grazing bifurcations from a period-1 attractor to a period-M attractor, with $M=3,4,\ldots$. In this case the actual bifurcation is a collision of an unstable period-M orbit and the period-1 orbit at $\rho=0$.

The purpose of this paper is to carry on a similar analysis for nonpositive values of the parameter α (only $\alpha>0$ was considered in [7]). For $\alpha<0$ the system has a stable period-1 orbit for negative ρ values, which becomes a flip saddle for positive ρ values up to $\rho=\rho_s\equiv 3/[4(1+\gamma\tau^2)]$. Here (as in [7]) the maximal periodic orbits (i.e., periodic orbits for which only one point per period is in the region $x>0$) are involved in the bifurcation at $\rho=0$.

Since both γ and τ^2 provide energy loss mechanisms, τ^2 is taken to be 1 for simplicity in the following. Thus Eq. (1) with $\gamma=1$ corresponds to a piecewise smooth symplectic map. Our strategy is to find necessary conditions for the existence of maximal periodic orbits, and the range of ρ values in which they are stable. Numerical experiments suggest, however, that these are also sufficient conditions.

II. ANALYSIS

For a maximal orbit of period M we can assume, without loss of generality, $x_1>0$, so that $x_2,x_3,\ldots,x_M$ are negative and $x_{M+1}=x_1$. The positions of the points along the trajectory can be obtained upon repeated iteration of Eq. (1), and are given by

$$x_{k+1}=\frac{1}{\sin\theta}\left[r^{k-1}(y_1-\sqrt{x_1})\sin k\theta-r^k x_1\sin(k-1)\theta+\rho\frac{\sin\theta-r^k\sin(k+1)\theta+r^{k+1}\sin k\theta}{1-\alpha+\gamma}\right], \tag{3}$$

$$y_{k+1}=\frac{1}{\sin\theta}\left[-r^k(y_1-\sqrt{x_1})\sin(k-1)\theta+r^{k+1}x_1\sin(k-2)\theta-r^2\rho\frac{\sin\theta-r^{k-1}\sin k\theta-r^k\sin(k-1)\theta}{1-\alpha+\gamma}\right], \tag{4}$$

with $k=1,2,\ldots,M$ and

$$r=\sqrt{\gamma},\quad \theta=\cos^{-1}\left[\frac{\alpha}{2r}\right]. \tag{5}$$

If we make $x_{M+1}=x_1$ and $y_{M+1}=y_1$ in Eqs. (3) and (4), we obtain two solutions for the coordinate x_1 of the maximal orbit:

$$\sqrt{x_{11}}=[-1+\sqrt{1-4C_x^MC_\rho^M\rho\gamma^{1-M}}]\frac{\gamma^{(M-1)/2}}{2C_x^M},$$

$$\sqrt{x_{12}}=[-1-\sqrt{1-4C_x^MC_\rho^M\rho\gamma^{1-M}}]\frac{\gamma^{(M-1)/2}}{2C_x^M}, \tag{6}$$

whereas for the coordinate y_1 we have

$$y_1=\frac{1}{\sin\theta+r^M\sin(M-1)\theta}\left[-\gamma\rho\frac{\sin\theta-r^{M-1}\sin M\theta+r^M\sin(M-1)\theta}{1-\alpha+\gamma}+r^M\sqrt{x_1}\sin(M-1)\theta+r^{M+1}x_1\sin(M-2)\theta\right]. \tag{7}$$

The general expressions for the coefficients C_x^M and C_ρ^M in Eq. (6) are given in [7] [Eqs. (38) and (39)], and will be written down in the following for each particular value of M considered.

From Eqs. (3) and (4) we can now construct the Jacobian matrix and the determinant D and the trace T of this matrix. D and T determine the eigenvalues λ_i and therefore the stability of the maximal periodic orbit via the expression

$$\lambda_{1,2}=\tfrac{1}{2}(T\pm\sqrt{T^2-4D}\,). \tag{8}$$

It can be shown that

$$D=\gamma^M,\quad T=-\frac{r^{M-1}}{\sin\theta}\left[\frac{1}{2\sqrt{x_1}}\sin M\theta+2r\sin(M-1)\theta\right]. \tag{9}$$

Note that since $\lambda_1\lambda_2=D$ and $D<1$ for $0<\gamma<1$, the only possible way for an eigenvalue to pass through the unit circle (to go from stable to unstable or vice versa) is either through $+1$ or through -1, i.e., no Hopf bifurcations can occur for maximal orbits. The condition that $\lambda=\pm1$, from Eq. (8), is

$$D \mp T + 1 = 0 , \tag{10}$$

which, once we have inserted Eqs. (9) and (6), gives us the value of the parameter ρ for which saddle-node ($\lambda = +1$) and/or flip bifurcations ($\lambda = -1$) take place for the maximal orbit.

With all these ingredients we are now ready to discuss the different kinds of maximal orbits and the bifurcations in the region of nonpositive α according to its period M.

(a) $M = 2$. In this case the coefficients in Eqs. (6) are given by

$$C_x^2 = \frac{1}{\alpha}\sqrt{\gamma}(1+\gamma)^2, \quad C_\rho^2 = -\frac{1}{\alpha}\sqrt{\gamma}(1+\alpha+\gamma) . \tag{11}$$

For $\alpha < 0$ we have $C_x^2 < 0$ and $C_\rho^2 > 0$. Therefore both solutions x_{11} and x_{12} can exist in the range $-2\sqrt{\gamma} < \alpha < 0$. Expressions (6) for $\sqrt{x_{11}}$ and $\sqrt{x_{12}}$ and Eq. (10) indicate that a pair of period-2 orbits are created in a saddle-node bifurcation at

$$\rho \equiv \rho_2 = \frac{\gamma}{4C_x^2 C_\rho^2} = \frac{-\alpha^2}{4(1+\gamma)^2(1+\alpha+\gamma)} < 0 . \tag{12}$$

The orbit corresponding to x_{11} only exists for $\rho < 0$, and collapses onto the point (0,0) as $\rho \to 0^-$, whereas the orbit corresponding to x_{12} continues to exist up to the value

$$\rho \equiv \rho_d = \frac{1}{1+\gamma} , \tag{13}$$

which is independent of α. At $\rho = \rho_d$ the periodic orbit is formed by the points $(x_1 = \rho_d^2, y_1 = 0)$ and $(x_2 = 0, y_2 = -\gamma x_1)$, i.e., it touches the axis $x = 0$. For $\rho > \rho_d$ it no longer exists, hence the orbit is destroyed upon crossing the boundary $x = 0$. This is a general property observed for the periodic orbits of the map (1). The situation is illustrated in the bifurcation diagram of Fig. 2, obtained for $\gamma = 0.8$ and $\alpha = -1.5$. In this case $\rho_2 \simeq -0.578$, $\rho_s \simeq 0.416$, and $\rho_d \simeq 0.555$.

It can be shown analytically that the maximal orbit corresponding to x_{12} is stable at $\rho = 0$, and no flip bifurcation is possible. Therefore we conclude that it is always stable, whereas the orbit corresponding to x_{11} remains unstable. This constitutes a difference with respect to the region $\alpha > 0$, where it can be shown that a flip bifurcation occurs to the stable branch for systems with $\gamma < 1$.

For the particular value $\gamma = 1$ the only difference is that, for the orbit corresponding to x_{12}, we have $\lambda_1 = \lambda_2^*$ on the unit circle (here λ_2^* denotes the complex conjugate of λ_2), and $\lambda_1 = \lambda_2^{-1} \in \mathbb{R}$ for x_{11}.

If $\alpha = 0$ the expressions (6) and (11) are no longer valid. Instead [from Eqs. (3) and (4)] we have a $M = 2$ maximal periodic orbit located at

$$x_1 = \frac{\rho}{1-\alpha+\gamma}, \quad y_1 = \frac{\gamma}{1+\gamma}(\sqrt{x_1} - \rho) \tag{14}$$

for $0 < \rho \le \rho_d$. This orbit can be shown to be stable. In this case there is a bifurcation from the stable period-1 orbit with coordinates

$$\left[x_f = \frac{\rho}{1-\alpha+\gamma}, y_f = -\gamma x_f \right] \tag{15}$$

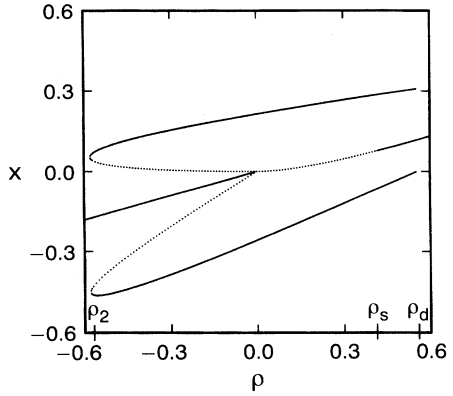

FIG. 2. Bifurcation diagram for $(\gamma, \alpha) = (0.8, -1.5)$. A stable period-2 maximal orbit and an unstable period-2 maximal orbit are created in a saddle-node bifurcation at $\rho = \rho_2 < 0$. The dashed curves indicate the locations of the unstable period-2 orbit for $\rho < 0$. The stable period-1 orbit and the stable period-2 orbit are on the solid curves. The unstable period-2 orbit collapses onto the stable period-1 orbit at $\rho = 0$. The stable period-2 trajectory is destroyed at the singularity axis $x = 0$. The period-1 orbit is unstable for $0 < \rho < \rho_s$ (dashed line for $\rho > 0$).

for $\rho < 0$ to a stable period-2 maximal orbit at $\rho = 0$. The unstable branch does not exist here.

(b) $M = 3$. Now the coefficients C_x^3 and C_ρ^3 are

$$\begin{aligned} C_x^3 &= \frac{\gamma}{\alpha^2 - \gamma}(1 + 2\alpha\gamma + \gamma^3) , \\ C_p^3 &= \frac{-\gamma}{\alpha^2 - \gamma}[\alpha^2 + (1+\gamma)\alpha + 1 + \gamma^2 - \gamma] . \end{aligned} \tag{16}$$

According to the sign of the product $C_x^3 C_\rho^3$ we can distinguish three cases for the analysis:

$$\begin{aligned} &\text{case (i):} \quad -2\sqrt{\gamma} < \alpha < \alpha_0 \equiv -\frac{1+\gamma^3}{2\gamma}, \\ &C_x^3 C_\rho^3 > 0, \quad C_x^3 < 0 , \\ &\text{case (ii):} \quad \alpha_0 < \alpha < -\sqrt{\gamma}, \quad C_x^3 C_\rho^3 < 0, \quad C_x^3 > 0 , \\ &\text{case (iii):} \quad -\sqrt{\gamma} < \alpha \le 0, \quad C_x^3 C_\rho^3 < 0, \quad C_x^3 < 0 \end{aligned}$$

Case (ii) does not exist for $\gamma = 1$. In order to analyze the conditions of existence of period-3 maximal orbits, explicit expressions for the points along the trajectory and the locations of its zeros are needed. Let us denote by

$$x_{21} = \frac{t_-(\rho)}{1+\alpha\gamma}, \quad x_{31} = \frac{s_-(\rho)}{1+\alpha\gamma} \tag{17}$$

and

$$x_{22} = \frac{t_+(\rho)}{1+\alpha\gamma}, \quad x_{32} = \frac{s_+(\rho)}{1+\alpha\gamma} \tag{18}$$

the x coordinates of the second and third points of the orbit corresponding to $\sqrt{x_{11}}$ and $\sqrt{x_{12}}$, respectively, with

$$t_{\pm}(\rho)=a\left[1\pm\left[1-\frac{\rho}{\rho_3}\right]^{1/2}\right]+b\rho\ , \tag{19}$$

$$s_{\pm}(\rho)=c\left[1\pm\left[1-\frac{\rho}{\rho_3}\right]^{1/2}\right]+d\rho\ , \tag{20}$$

and

$$a=\frac{\gamma}{2C_x^3}\left[1+\frac{\gamma^3}{C_x^3}\right],\quad b=1-\gamma-\gamma^2\frac{C_\rho^3}{C_x^3},\quad \rho_3=\frac{\gamma^2}{4C_\rho^3C_x^3}\ , \tag{21}$$

$$c=\frac{\gamma}{2C_x^3}\left[\alpha-\frac{\gamma^2}{C_x^3}\right],\quad d=1+\alpha+\gamma\frac{C_\rho^3}{C_x^3}\ . \tag{22}$$

Then a simple calculation shows that

$$\rho=\rho_u(\alpha)\equiv-\frac{a}{b}\left[2+\frac{a}{b\rho_3}\right] \tag{23}$$

is a solution of $x_{22}=0$ if $u_2\equiv1+(a/b\rho_3)>0$, whereas, in addition to $\rho=0$, $\rho=\rho_u$ is a solution of $x_{21}=0$ only if $u_2<0$. Concerning the third point of the orbit, analogously,

$$\rho=\rho_v(\alpha)=-\frac{c}{d}\left[2+\frac{c}{d\rho_3}\right], \tag{24}$$

is a zero of x_{32} if $u_3\equiv1+(c/d\rho_3)>0$, whereas if $u_3<0$, the solutions of the equation $x_{32}=0$ are given by $\rho=0$ and $\rho=\rho_v$.

A careful analysis of all these functions in the physical region of parameters allows us to conclude the following:

(b1) For case (i) both solutions x_{11} and x_{12} given by Eq. (6) are real for $\rho\geq0$, so in principle maximal orbits corresponding to $\sqrt{x_{11}}$ and $\sqrt{x_{12}}$ may exist up to $\rho=\rho_3>0$, whereas for $\rho\leq0$ only the solution x_{12} is real. It turns out, however, that the only existing period-3 maximal orbit is that corresponding to $\sqrt{x_{12}}$. It exists for $-\infty<\rho\leq\rho_u$, for systems with (γ,α) in the region

$$-2\sqrt{\gamma}<\alpha<1-\gamma-\frac{1}{\gamma}<\alpha_0\ . \tag{25}$$

In all other cases x_{21} and x_{22} are positive. (At the particular value $\alpha=1-\gamma-(1/\gamma)$, the coefficient $b=0$, and u_2 changes sign). The orbit corresponding to $\sqrt{x_{12}}$ is always unstable, with real eigenvalues $\lambda_1>1$ and $0<\lambda_2<1$. At $\rho=\rho_u$ with $\rho_u\neq0$, the orbit points of the periodic trajectory are

$$\left[x_{12}=\frac{(\alpha+1)\rho_u}{1+\alpha\gamma},y_{12}>0\right],\quad(x_{22}=0,y_{22}=-\gamma x_{12})\ ,$$

$$(x_{32}=-\gamma x_{12}+\rho_u<0,y_{32}=0)\ ,$$

so that one point of the orbit lies on the singularity axis $x=0$. The terminal value ρ_u is positive for α in the interval $]-2\sqrt{\gamma},-1/\gamma[$ and negative for α in $]-1/\gamma,1-\gamma-(1/\gamma)[$, whereas for parameter values on the line $\alpha=-1/\gamma$ this period-3 maximal orbit disappears at $\rho=0$, i.e., at grazing. In this case the corresponding expression for x_{12} is given by

$$x_{12}=[1+\sqrt{1-4(1-\gamma)\gamma^2\rho}]^2\frac{1}{4\gamma^4}\ . \tag{26}$$

Figure 3 shows the x projection of this unstable $M=3$ maximal periodic orbit for $\gamma=0.7$ and $\alpha=-1.5$ as a function of ρ. For these values $\rho_u\simeq0.3698$ and $\rho_3\simeq1.6192$.

(b2) For case (ii) no period-3 maximal orbit exists, regardless of the value of ρ. The coordinate x_{21} of the orbit corresponding to x_{11}, the only real solution in this case, is always positive.

(b3) For case (iii), both solutions x_{11} and x_{12} are real for ρ in the interval $]\rho_3,0[$, and only x_{12} is real for $\rho>0$. Thus the periodic orbit corresponding to x_{11} can exist, in principle, for $\rho<0$, whereas the orbit corresponding to x_{12} can also exist for ρ positive. Nevertheless, it can be shown that x_{2i} and x_{3i} $(i=1,2)$ are not simultaneously negative for $\alpha\leq-\gamma$. Only for $\alpha>-\gamma$ the x coordinates of the second and third points are negative and period-3 maximal orbits exist. More specifically, let α_v be the value of α in the interval $]-\gamma,-\gamma^2[$ such that $\rho_v(\alpha_v)=\rho_3<0$. Then it can be shown that

(i) For $\alpha<\alpha_v$ (between the curves $\alpha=-\gamma$ and $\alpha=-\gamma^2$), then $\rho_3<\rho_v<0<\rho_u$, and only the orbit corresponding to x_{11} exists in the range $\rho\in[\rho_v,0[$. It is created at $\rho=\rho_v$ on the border $x=0$ and is unstable. This orbit collapses onto the origin as $\rho\to0^-$. For $\rho_3<\rho<\rho_v$ there are no $M=3$ maximal orbits. In Fig. 4(a) we plot this periodic trajectory for $\gamma=0.5$ and $\alpha=-0.48$. In this case $\alpha_v\simeq-0.4262$, $\rho_3\simeq-0.1082$, and $\rho_v\simeq-0.0631$.

(ii) If $\alpha=\alpha_v$ then the range of existence of the unstable orbit corresponding to x_{11} is $[\rho_v=\rho_3,0[$.

(iii) For $\alpha_v<\alpha\leq0$ (above the curve $\alpha=-\gamma$) a pair of period-3 maximal orbits are created in a saddle-node bifurcation at $\rho=\rho_3$. The orbit corresponding to x_{11} is unstable, and exists up to $\rho=0$, at which point it collapses on to the origin $(x=y=0)$. The stable orbit correspond-

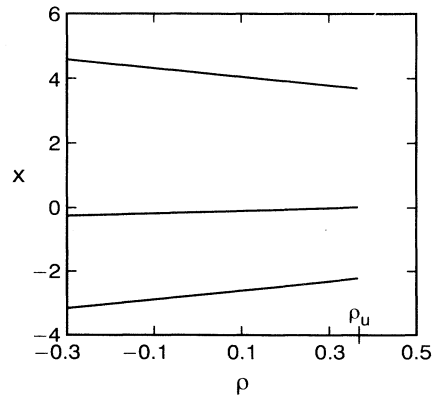

FIG. 3. Unstable period-3 maximal orbit corresponding to x_{12} for $\gamma=0.7$ and $\alpha=-1.5$, in the region $\alpha<1-\gamma-(1/\gamma)$. The orbit is destroyed when one of its points touches the singularity axis $x=0$ at $\rho=\rho_u$.

ing to x_{12} only exists up to $\rho=\rho_v$, where one of its points (x_{32}) lies on the axis $x=0$. The sign of ρ_v depends on the values of α considered. Thus, for $\alpha<-\gamma^2$, then $\rho_v<0$, and the stable orbit disappears before the unstable one. When $\alpha=-\gamma^2$, then $\rho_v=0$ and the orbit disappears at grazing, whereas $\rho_v>0$ for $-\gamma^2<\alpha\leq 0$. Figure 4(b) shows a typical bifurcation diagram for (γ,α) in this region of parameters. It is worth noting here that, in a similar way to the case $M=2$, no flip bifurcations are possible for $M=3$ maximal orbits.

(c) $M=4$. A similar analysis carried out for period-4 maximal orbits leads to the conclusion that they are not present in the system for $\alpha\leq 0$. This result supports the claim made in Ref. [7] that at most two regions in the parameter space corresponding to maximal orbits of different periods can overlap, and allows us to conclude that no maximal orbits with period $M\geq 4$ can exist for $\alpha\leq 0$.

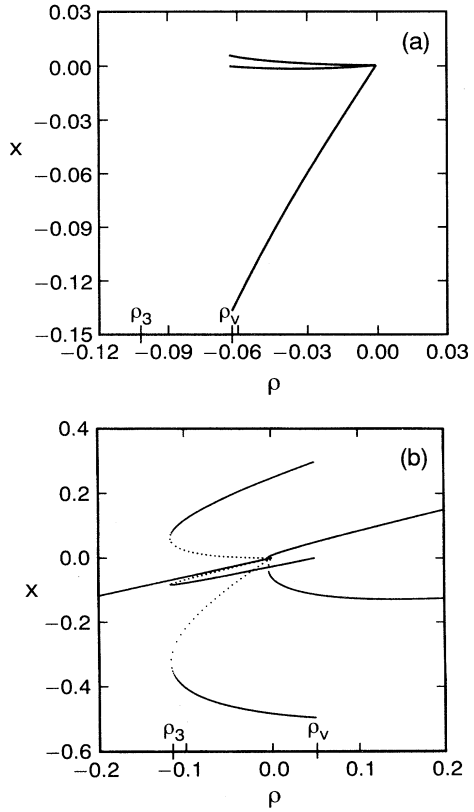

FIG. 4. (a) Unstable period-3 maximal orbit corresponding to x_{11} for $\gamma=0.5$, and $-\gamma<\alpha=-0.48<\alpha_v$. It is created at $\rho=\rho_v>\rho_3$ on the border $x=0$ and collapses onto the origin as $\rho\to 0^-$. (b) Bifurcation diagram for $\gamma=0.5$, and $-\gamma^2<\alpha=-0.2<0$. A pair of period-3 maximal orbits are created in a saddle-node bifurcation at $\rho=\rho_3<0$. One of them (solid curve) is stable, and the other (dashed curve) is unstable. The stable period-3 maximal orbit is destroyed at $\rho=\rho_v>0$. A stable period-2 maximal orbit and an unstable period-2 maximal orbit are created at $\rho=\rho_2<0$ in a saddle-node bifurcation. The unstable period-2 and -3 maximal orbits collapse onto the stable period-1 orbit at $\rho=0$.

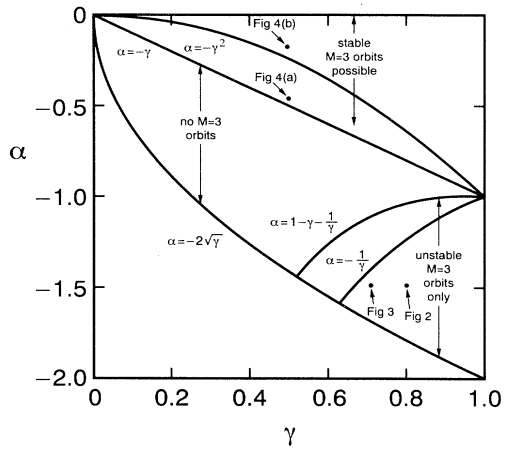

FIG. 5. Regions of the (γ,α) parameter space corresponding to the different cases analyzed in the paper for the Nordmark map. Only the region $\alpha>-2\sqrt{\gamma}$ represents physical systems.

III. SUMMARY AND CONCLUSIONS

We summarize the above results in Fig. 5, which shows the regions in the parameter space (γ,α) corresponding to the different cases previously analyzed. The parameter values corresponding to Figs. 2–4 are labeled as points. Only parameter values above the curve $\alpha=-2\sqrt{\gamma}$ represent physical situations (positive friction). In all this region there are two maximal orbits of period $M=2$. They are created in a saddle-node bifurcation, and the unstable branch collides with the period-1 attractor at grazing. The curves $\alpha=1-\gamma-(1/\gamma)$ and $\alpha=-\gamma$ are the boundary of the two regions where period-3 maximal orbits appear. For $\alpha<1-\gamma-(1/\gamma)$ the $M=3$ orbits are unstable, whereas for $\alpha>-\gamma$ it is also possible to have stable trajectories.

When the parameters (γ,α) are in the region where period-2 and -3 stable maximal orbits coexist (i.e., for $\alpha>\alpha_v$, above the curve $\alpha=-\gamma$), at $\rho=0$ we have a collision of the unstable $M=2$ and 3 orbits created at ρ_2 and ρ_3, respectively ($\rho_3<\rho_2<0$), with a period-1 stable attractor. The result is that it is always the maximal stable orbit of period 2 that the orbit goes to from the fixed point as ρ increases from negative to positive values. As an example of what happens in this region of parameters, in Fig. 4(b) we represent the bifurcation diagram of the Nordmark map for $(\gamma=0.5,\alpha=-0.2)$. Here the grazing effect consists in the collision of a period-3 and a period-2 unstable maximal orbit with a period-1 attractor at $\rho=0$, with the result that a bifurcation from a stable fixed point to a stable period-2 maximal orbit is observed in the bifurcation diagram.

For α in the range $]-\gamma,\alpha_v]$ the grazing effect consists in the collision of a period-2 and a -3 unstable maximal orbits with a fixed point at $\rho=0$. Finally, for $\alpha<1-\gamma-(1/\gamma)$ the only $M=3$ maximal orbit is unstable and disappears when one of its points reaches the singularity axis $x=0$.

In addition to these, other interesting phenomena not observed in the region of positive α are produced at graz-

ing for some parameter values. In particular, on the curve $\alpha = -\gamma^2$ not only the unstable $M = 3$ maximal orbit is destroyed at $\rho = 0$, but also the stable one. This also happens to the unstable period-3 orbit for $\alpha = -(1/\gamma)$.

In summary, we have completed the analysis of the role that maximal periodic orbits play in the bifurcations of a piecewise smooth map which captures the universal properties of impact oscillators near grazing. We have shown the existence of interesting phenomena in the physical region of parameters for $\alpha < 0$, and clarified how periodic orbits are created and destroyed in the system. More specifically, a maximal periodic orbit is destroyed when one of its points reaches the singularity axis $x = 0$. Unstable maximal orbits can also be created at the border $x = 0$ for some values of the parameters, whereas stable trajectories are always created in a saddle-node bifurcation (with an unstable orbit) for some negative value of ρ. Neither Hopf nor flip bifurcations occur for maximal orbits.

Besides maximal orbits, other kinds of stable periodic orbits with multiple impacts also exist in the system with $\alpha < 0$. In particular, period-3 and -5 orbits with two impacts per period have been detected. The latter, in the same way as maximal orbits, are created in a saddle-node bifurcation at some $\rho < 0$ and destroyed at the border $x = 0$, whereas period-3 orbits are destroyed at some positive ρ in a saddle-node bifurcation and apparently exist for all $\rho < 0$.

ACKNOWLEDGMENTS

The work of F.C. has been supported by a grant from the Conselleria de Educació de la Generalitat Valenciana (Spain), and by the collaboration program UJI-Fundació Caixa Castelló 1994. This work was also supported by the Department of Energy (Office of Scientific Computing).

[1] S. W. Shaw and P. J. Holmes, J. Sound Vib. **90**, 129 (1983).
[2] S. W. Shaw, ASME J. Appl. Mech. **52**, 453 (1985).
[3] S. Foale and S. R. Bishop, Philos. Trans. R. Soc. London Ser. A **338**, 547 (1992).
[4] C. Budd and F. Dux, Nonlinearity **7**, 1191 (1994).
[5] C. Budd, F. Dux, and A. Cliffe, J. Sound Vib. **184**, 475 (1995).
[6] A. B. Nordmark, J. Sound Vib. **145**, 279 (1991).
[7] W. Chin, E. Ott, H. E. Nusse, and C. Grebogi, Phys. Rev. E **50**, 4427 (1994); Phys. Lett. A **201**, 197 (1995).
[8] H. E. Nusse and J. A. Yorke, Physica D **57**, 39 (1992).